

Practical Aspects of Sample Preparation and Setup of ^1H $R_{1\rho}$ Relaxation Dispersion Experiments of RNA

Hannes Feyrer¹, Judith Schlagnitweit¹, Katja Petzold¹

¹Department of Medical Biochemistry and Biophysics, Karolinska Institutet

Corresponding Author

Katja Petzold
katja.petzold@ki.se

Citation

Feyrer, H., Schlagnitweit, J., Petzold, K. Practical Aspects of Sample Preparation and Setup of ^1H $R_{1\rho}$ Relaxation Dispersion Experiments of RNA. *J. Vis. Exp.* (173), e62470, doi:10.3791/62470 (2021).

Date Published

July 9, 2021

DOI

10.3791/62470

URL

jove.com/video/62470

Abstract

RNA is a highly flexible biomolecule, wherein changes in structures play crucial roles in the functions that RNA molecules execute as cellular messengers and modulators. While these dynamic states remain hidden to most structural methods, $R_{1\rho}$ relaxation dispersion (RD) spectroscopy allows the study of conformational dynamics in the micro- to millisecond regime at atomic resolution. The use of ^1H as the observed nucleus further expands the time regime covered and gives direct access to hydrogen bonds and base pairing.

The challenging steps in such a study are high-purity and high-yield sample preparation, potentially ^{13}C - and ^{15}N -labeled, as well as setup of experiments and fitting of data to extract population, exchange rate, and secondary structure of the previously invisible state. This protocol provides crucial hands-on steps in sample preparation to ensure the preparation of a suitable RNA sample and setup of ^1H $R_{1\rho}$ experiments with both isotopically labeled and unlabeled RNA samples.

Introduction

RNAs perform a multitude of regulatory¹, catalytic², and structural³ functions in the cell, many of which are correlated to a flexible molecular structure and intricate changes of those structures^{4,5,6,7}. Low-populated states remain invisible to most methods of structure determination or do not allow the study of these hidden states at high atomic resolution. Solution-state nuclear magnetic resonance

(NMR) spectroscopy combines both aspects by providing access to individual atomic nuclei as well as offering a large toolbox of experiments targeting dynamics through all time regimes⁸. RD NMR experiments provide access to conformational exchange in the intermediate timescale, wherein changes in base pairing patterns and local structural rearrangements can be expected^{5,9,10,11,12,13,14}. RD experiments are performed as long R_2 measurements in the form of a Carr-Purcell-Meiboom-Gill pulse train¹⁵ or as

relaxation measurements in the rotating frame, called $R_{1\rho}$ RD experiments¹⁶.

Although both can be used to extract population of and exchange rate and chemical shift difference to the minor state, $R_{1\rho}$ RD experiments also give the sign of the chemical shift difference of the excited state. This allows an inference on secondary structure, which strongly correlates to chemical shift in RNA structures¹⁷. The chemical shift is a good indicator of helicity in the case of aromatic protons and carbons on the nucleobases, of base pairing partners for imino protons, and of sugar puckers on the C4' and C1' atoms^{18,19}. It should be noted that recently a chemical exchange saturation transfer (CEST) experiment using higher spin lock (SL) power, thereby shifting the applicability of the CEST experiment to faster exchange timescales, was published as an alternative to the $R_{1\rho}$ RD experiment for systems with one excited state.

Although ^{13}C and ^{15}N isotopes have often been used to access structural exchange, recent work from this laboratory used aromatic and imino protons as probes for conformational exchange^{9,10}. The use of ^1H as the observed nucleus brings several advantages, for example, access to exchange on faster and slower timescales, higher sensitivity, and shorter measurement times. This is further facilitated by the SElective Optimized Proton Experiment (SELOPE) approach, providing access to aromatic protons through decrowding of the one-dimensional (1D) spectrum using homonuclear scalar couplings, instead of a heteronuclear magnetization transfer, and eliminating the need for isotope labels²⁰. This protocol addresses the measurement in ^1H $R_{1\rho}$ RD experiments of uniformly $^{13}\text{C}/^{15}\text{N}$ -labeled and unlabeled samples. Therefore, this paper presents a sample preparation method that was found to be the most versatile

for different sample preparation needs²¹ and discusses alternatives in the last section of this article (**Figure 1**).

At this point, the reader should note that other sample preparation techniques are acceptable for ^1H $R_{1\rho}$ RD experiments, and that other methods of structural and functional analysis can be performed with the samples synthesized with the presented technique. ^1H $R_{1\rho}$ RD experiments require high RNA concentrations (ideally >1 mM) as well as high homogeneity, both in RNA length and structural conformation to ensure reliable characterization of molecular dynamics. *In vitro* transcription (IVT) is the method of choice for many researchers to produce $^{13}\text{C}/^{15}\text{N}$ -labeled RNA samples due to the availability of labeled nucleoside triphosphates (NTPs) and facile incorporation in the enzymatic reaction²². However, the widely used T7 RNA polymerase (T7RNAP)^{23,24,25} suffers from low 5' homogeneity in case of certain initiation sequences^{26,27} and often also 3' homogeneity during transcription runoff²⁸. Purification of the target RNA species becomes more expensive and laborious due to the need of large quantities of ~ 200 nmol. The method used here has been presented previously where advantages were discussed at large²¹. In brief, it solves described issues by transcribing a larger tandem transcript that is then site-specifically cleaved by *Escherichia coli* RNase H, guided by a chimeric oligonucleotide^{29,30} (see **Figure 2** for details).

Incorporation of a spacer sequence at the 5' and 3' ends of the tandem transcript allows the use of a high-yield initiation sequence and removal of terminal overhangs close to the linearization site of the plasmid template, respectively (**Figure 2B**). The method was shown to improve yields significantly, while reducing cost and labor, with the caveat of a more complex template synthesis and the need for an

additional enzyme and oligonucleotide. The high specificity of RNase H cleavage facilitates purification due to the lack of RNA species in a similar size range. The present protocol uses an ion exchange high-performance liquid chromatography (HPLC) step that has been published by this laboratory recently³¹, although other methods are possible alternatives. ^1H $R_{1\rho}$ RD can, in general, be acquired on labeled or unlabeled samples with two respective pulse sequences, the “labeled” ^1H $R_{1\rho}$ heteronuclear single quantum correlation (HSQC)-based experiment with a ^{13}C indirect dimension¹⁰ and the “unlabeled” ^1H $R_{1\rho}$ SELOPE-based experiment with a ^1H indirect dimension²⁰.

These two-dimensional (2D) experiments can serve as a first check, regardless of whether dynamics on the $R_{1\rho}$ timescale are present in the sample. An overview of RD for all resolved peaks in the spectra can be obtained, and peaks of interest for a more thorough RD analysis can be identified. This means that even unlabeled samples can be checked before a decision to produce a more expensive, labeled sample is made. Once a peak with conformational exchange contribution is selected to be studied more thoroughly, it is best to switch to the 1D versions of the above experiments (if the peak can still be resolved) to carry out so-called off-resonance experiments. For the labeled version, the HSQC transfer to ^{13}C is replaced with

a selective heteronuclear cross-polarization (HCP) step as used in ^{13}C $R_{1\rho}$ experiments^{32,33,34,35}, while in the case of the SELOPE experiment, the experiment is simply run as a 1D, which is especially useful for H8 and H2 signals that are lying on the diagonal in the 2D anyway. One criterion as to which sequence to use, provided that both, a labeled as well as unlabeled sample are available, is how well isolated the peak of interest is in the two experiments.

In general, the SELOPE experiment is recommended for RNA samples of up to 50 nucleotides. For larger RNAs, the overlap will be bigger; however, structurally interesting nucleotides often appear in chemical shift regions that are less overlapped and still might be accessible in even larger RNAs. Another argument would be that in unlabeled samples, no J-coupling occurs between ^1H and ^{12}C . However, as the minimum spin lock power is defined by the minimum power used to decouple those two spins (~ 1 kHz) in the labeled experiment, the unlabeled experiment allows the use of a broader range of spin lock (SL) strengths and therefore, access to a broader timescale of exchange. These off-resonance experiments provide additional information to k_{ex} , such as population of the excited state (alternative conformer), p_{ES} , as well as very valuable chemical shift information in the form of $\Delta\omega$ (the chemical shift difference of the ground state and the excited state).

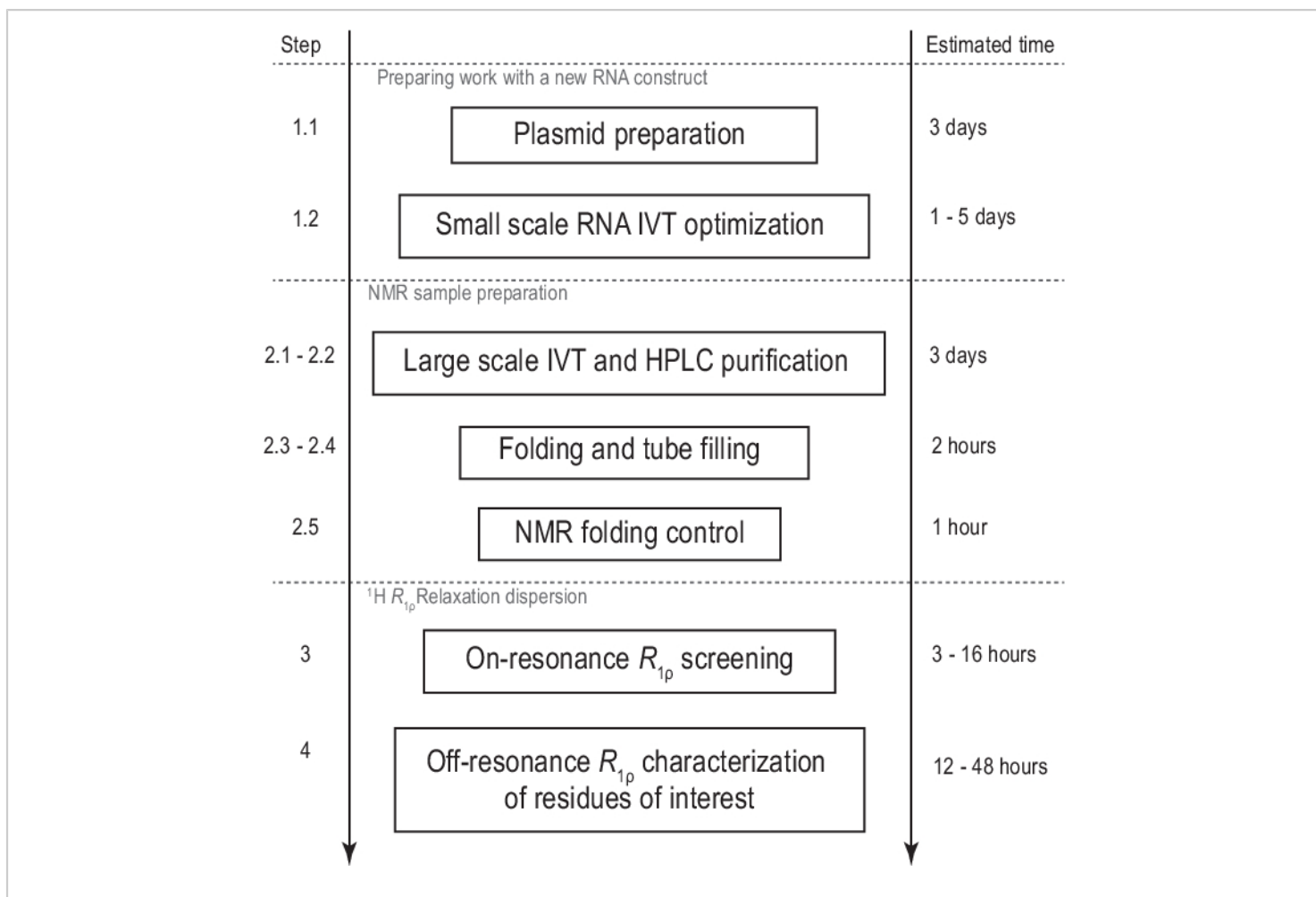


Figure 1: Workflow of the presented protocol. Preparation before the actual large-scale sample production, consisting of template preparation and confirmation of successful *in vitro* transcription and RNase H cleavage. Large scale production including HPLC purification, filling of NMR tube, and confirmation of RNA folding. In case of isotope-labeled synthesis, an unlabeled purification should be performed for gradient optimization on the same day. NMR characterization of conformational dynamics with $R_{1\rho}$ experiments. Each step can be performed independently, e.g., the $^1\text{H } R_{1\rho}$ RD analysis can be applied to any suitable RNA sample produced with another method. Abbreviations: IVT = *in vitro* transcription; HPLC = high-performance liquid chromatography; NMR = nuclear magnetic resonance; RD = relaxation dispersion. [Please click here to view a larger version of this figure.](#)

The aim of this protocol is to provide practical details and critical parameters for the study of conformational dynamics with $^1\text{H } R_{1\rho}$ relaxation dispersion in RNA hairpin molecules. After providing a detailed protocol of the design, synthesis, and ion exchange HPLC purification of a target RNA that can

be performed using all, some, or none NTPs as $^{13}\text{C}/^{15}\text{N}$ -labeled versions, the workflow of finalizing the NMR sample and confirming the conformational exchange with NMR spectroscopy has been described. Finally, the details for the setup of $^1\text{H } R_{1\rho}$ RD experiments on a Bruker NMR

spectrometer are described (**Figure 1**). The protocol gives each step to set up the 1D version for labeled samples and additional comments and a table to adjust for the setting up of the SELOPE version (**Table 2**). After the protocol, critical

steps and alternative routes to sample preparation and ^1H $R_{1\rho}$ RD setup are discussed.

Protocol

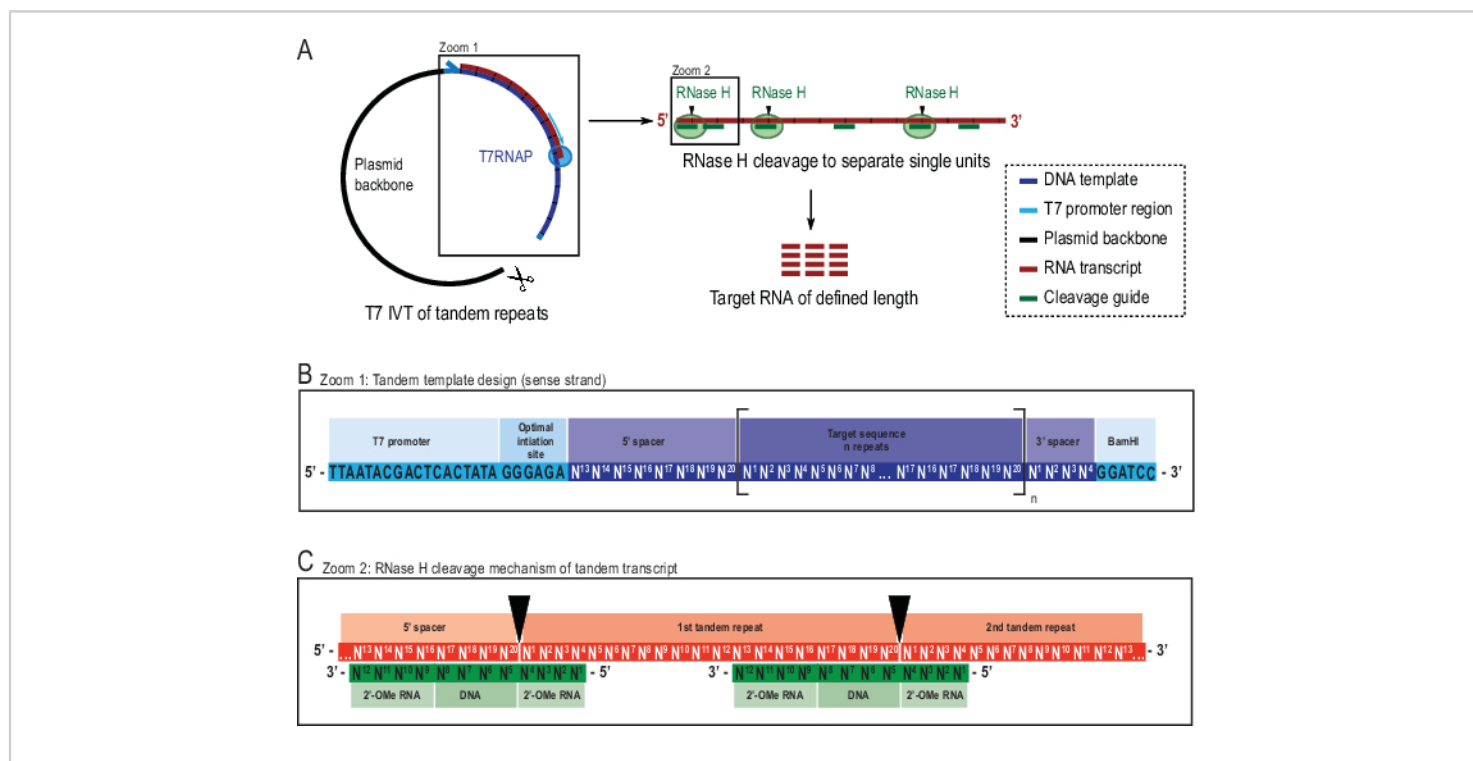


Figure 2: Schematic representation of the reported tandem IVT protocol. (A) Tandem transcription from a linearized plasmid template with T7RNAP (left) and successive cleavage by RNase H of the transcript to achieve target length RNA, directed by a chimeric DNA guide (right). (B) Detailed schematic of the tandem template starting with the viral T7RNAP promoter, an initiation sequence. The target sequence (dark blue, example here is 20 nt long) is repeated “n” times. The repeats flanked by a 5’ and 3’ spacer sequences consisting of the last eight and first four nucleotides, respectively, to allow for removal of the initiation and restriction sequences from the first and last repeat unit. (C) Hybridization of the tandem transcript (red) and the chimeric cleavage guides (green). RNase H cleaves the RNA opposite to the DNA 5’ end. The 2’-OMe RNA flanks increase specificity by enhancing the binding affinity of cleavage guide to the target RNA. This figure has been modified from ²¹. Abbreviations: T7RNAP = T7 RNA polymerase. [Please click here to view a larger version of this figure.](#)

1. Preparing work for a new RNA construct

1. Plasmid design and preparation

1. Write the template sequence in a cloning tool, e.g., Serial Cloner.

2. Take the T7 promotor sequence and add a high-yield initiation sequence (T7: 5'-TAATACGACTCACTATA[^]GGGAGA-3').

NOTE: Transcription will start at the nucleotide indicated with a caret (^). The initiation sequence GGGAGA is variable, but strongly sequence-dependent; therefore, the use of this sequence is recommended.

3. Add the last 8 nucleotides (nt) of the target sequence as a 5' spacer (5'S).
4. Add repeats of the target sequence (TS).
5. Add the first four nucleotides as a 3' spacer after the repeats (5'S).
6. Add a BamHI restriction site (RS) or similar unique restriction site.

NOTE: The total sequence as shown will be cloned or readily ordered in a bacterial high-copy plasmid (e.g., pUC19): 5'-T7-5'S-(TS)_n-3'S-RS-3' (**Figure 2B**). The number of repeats should be as high as allowed by gene synthesis (a maximum of 600 nt in this protocol).

7. Amplify the plasmid in *E. coli* using a commercial kit.
8. Linearize the purified plasmid at 20 ng/μL using the appropriate restriction site. Scale restriction digests with BamHI by up to 1 mL.
9. Purify the digested plasmid, and confirm successful linearization on a 1% agarose gel. Store the linearized plasmid at -20 °C for several months.

2. Cleavage guide design (**Figure 2C**)

1. Write the last eight nucleotides of the target RNA sequence in the 5'-3' direction, and add the first four

nucleotides of the target RNA sequence on the 3' end also in the 5'-3' direction.

2. Generate the reverse DNA complement of that sequence
3. Change the first and last four nucleotides to their 2'-OMe modifications by adding an 'm' before the nucleotide letter.

NOTE: For synthesis, mU is used instead of mT.

4. Order the oligo with standard desalting purification.
- NOTE:** Check if the generated oligo could bind at another place other than the connection of two RNA sequences. Full complementarity in the central four DNA nucleotides is required, while the flanking regions could permit a mismatch. If necessary, extend the flanks to up to 18 nt to generate a unique binding sequence³⁶.

3. Small-scale IVT

NOTE: For RNase-free work, prepare all reagents under sterile and RNase-free conditions. Use RNase decontamination reagent (see the **Table of Materials**) and 95% v/v ethanol to clean work surfaces and pipettes before use. Wash gloves with 95% ethanol and wear lint-free long-sleeved clothes. To minimize RNase contamination, do not breathe over open tubes.

1. Prepare stock solutions of Tris-Cl (pH 8.0), dithiothreitol, MgCl₂, spermidine, and NTPs/GMP (unbuffered). Mix reagents as shown in **Table 1**. Prepare a master mix of these reagents in advance, before the addition of enzymes or nucleic acids.

NOTE: If using frozen reagents, thoroughly mix them after thawing. Reagents might precipitate if mixed at too high concentrations, so it is strongly recommended to follow the order in **Table 1**.

- Add in the following order: plasmid, cleavage guide, inorganic phosphatase (iPPase), RNase H, T7RNAP. As enzyme activity might vary for enzymes produced in-house, test several concentrations before selecting the best one.

NOTE: Include a negative control for the cleavage reaction, *e.g.*, without RNase H, to attribute a missing target band to flawed RNase H cleavage and not to unsuccessful transcription.

- Incubate the reaction at 37 °C for 1 h and confirm reaction on a denaturing polyacrylamide

gel electrophoresis (PAGE) (**Figure 3A**). Dilute the sample 10-fold in loading solution, and load 1 μL onto the gel.

NOTE: Gel mixture: 8 M urea, 20% acrylamide (19:1 acrylamide:bisacrylamide) in 1x TBE. Loading solution: 5 mM ethylenediamine tetraacetic acid (EDTA), 300 μM bromophenol blue in formamide. RNase H cleavage reactions cannot be expected to be complete after 1 h, as new RNA is produced constantly. At this point, look out for a clear target band and the absence of a species of similar molecular weight (*e.g.*, ± 3 nucleotide (nt) products).

Reagent	Stock concentration	Amount small scale (μL)
H ₂ O	-	24
Tris	1 M	5
MgCl ₂	1 M	0.5
DTT	1 M	0.5
Spermidine	250 mM	5
GMP	100 mM	2.5
ATP	100 mM	1.5
GTP	100 mM	1.5
UTP	100 mM	1.5
CTP	100 mM	1.5
Plasmid	20 ng/ μL	5
Cleavage guide	100 μM	10
iPPase	10 mg/mL	0.5
RNase H	10 $\mu\text{g/mL}$	2
T7 RNA polymerase	5 mg/mL	2

Table 1: Reagent table for tandem IVT and simultaneous RNase H cleavage. Stock concentrations can be adapted to the user's convenience. If RNase H cleavage must be performed after T7 IVT, add cleavage guide and RNase H after heat-

inactivation of T7RNAP. Amounts used scale linearly with reaction scale. Abbreviations: T7RNAP = T7 RNA polymerase; IVT = *in vitro* transcription.

2. NMR sample preparation

1. Scale up the reaction to the desired volume (typically 10 mL), and run the reaction overnight. Test for reaction completion the next day with a denaturing PAGE gel (**Figure 3A**).

NOTE: Incomplete cleavage reaction is shown by higher molecular weight species above the target band.

1. If cleavage was not successful or complete, reanneal RNA and the cleavage guide in the reaction vessel by heating the solution in a conventional microwave at 450 W for 15 s.
2. Cool the solution slowly to 37 °C for 40 min. Use a heating block for volumes below 1 mL. Note the formation of new precipitate.
3. Add more IPPase and RNase H, and incubate for another 1-3 h at 37 °C. Confirm completion of the cleavage reaction with denaturing PAGE.
4. When the RNase H cleavage reaction is completed, quench the reaction by adding EDTA to 50 mM final concentration and vortex thoroughly.

NOTE: Potential pyrophosphate precipitation will dissolve, and new protein precipitate forms.

5. Filter the solution through a 0.2 µm syringe filter, and concentrate to a volume injectable into an HPLC system, depending on the injection loop size.

NOTE: The protocol can be paused here by freezing sample at -20 °C.

2. Large-scale HPLC purification

1. Prepare ion-exchange buffers A and B within one week of use. Filter and degas the buffers.

NOTE: Buffer A: 20 mM sodium acetate; 20 mM sodium perchlorate, pH 6.5. Buffer B: 20 mM sodium acetate; 600 mM sodium perchlorate, pH 6.5.

2. Equilibrate the column with 100% buffer B followed by 100% buffer A for at least 2 column volumes at 75 °C.

3. Prepare the HPLC sequence (**Figure 3B**) at a flow rate of 5.5 mL/min. Use the following sequence for purification of an RNA sized between 20 and 30 nt: 0-7 min: 0% B; 7-16 min: gradient 0-20% B; 16-46 min: elution, typically with a gradient of 20-30% B (optimize according to needs); 46-62 min: 100% B; 62-73 min: 0% B.

NOTE: A change in flow rate from 5.5 to 8 mL/min did not influence the separation in this protocol.

4. Optimize the elution gradient by the injection of an equivalent to 1 mL of transcription reaction (unlabeled) at a time.

NOTE: For further details and discussion, refer to Karlsson et al.³¹ and Feyrer et al.²¹.

5. Test the collected fractions on a denaturing PAGE. If the main elution peak is well isolated and contains the pure target RNA, scale up the purification to an equivalent of 10 mL of transcription reaction.

6. Collect the fractions of interest, concentrate, and exchange the buffer with NMR buffer. Use an ultracentrifugal filter unit (see the **Table of Materials**) for volumes above 50 mL.

NOTE: NMR buffer: 15 mM sodium phosphate; 25 mM sodium chloride; 0.1 mM EDTA, pH 6.5. To minimize loss from RNA adhering to plastic tube walls, wash all collection tubes with 1 mL of water, vortex, and centrifuge to collect all liquid.

7. Determine the concentration via ultraviolet spectroscopy. Calculate the reaction yield according to Feyrer et al²¹.

NOTE: The concentration of an NMR sample for RD experiments should not be below 130 nmol, which corresponds to 500 μ M in a sample volume of 250 μ L using NMR tubes (**Table of Materials**).

3. Folding of an RNA sample

1. Dilute and aliquot the sample of a volume of ~10 mL into 1 mL per tube.
2. Heat the RNA aliquots to 95 °C for 5 min.
3. Snap-cool the samples by placing them on ice or in a water-ice-salt mixture and incubate for 30 min.
4. Pool samples and concentrate to ~250 μ L in a 2 mL centrifugal filter unit.

4. Filling of an NMR tube

1. Clean the NMR tube in the NMR tube cleaner by flushing with abundant water, RNase decontamination reagent, water, 95% ethanol (EtOH), and water again. Leave to dry.
2. Clean the plunger by rinsing with water and wiping with RNase decontamination reagent and 95% EtOH using a lint-free wipe. Leave to dry.
3. Add 10% (v/v) of D₂O to the NMR sample.

4. Fill the RNA sample into the NMR tube using a large pipette tip. Let the liquid flow along the side of the tube wall.
5. Insert the plunger and remove air bubbles by pushing the plunger down together with a fast twisting motion.
6. Pull the plunger up slowly without creating new air bubbles and fix it with paraffin wax film.

5. Confirm folding by NMR.

NOTE: At this point, it is necessary to perform at least partial resonance assignment to confirm the secondary structure of the RNA sample and to identify regions of interest for the study of conformational dynamics. An exhaustive description on RNA resonance assignment would exceed this protocol, therefore we refer to well-established literature at this point^{19,37,38}. An electrophoretic mobility shift assay (EMSA) can be a helpful indicator of RNA folding and serve as complementary data for NMR experiments.

1. Compare the following spectra of the sample for which ¹H R₁ ρ RD experiments are performed with the properly folded reference sample (**Figure 4**): ¹H 1D, especially the imino region 10–15 ppm; Aromatic ¹H,¹³C-HSQC; ¹H,¹H-SELOPE (optional).

NOTE: An aromatic fingerprint is also necessary, even in case of agreement between imino signals, because dimer formation often shows the same or similar imino signals as an RNA hairpin. The SELOPE experiment can replace an ¹H,¹³C-HSQC for aromatic fingerprinting, as heteronuclear experiments on unlabeled samples are very time-consuming.

2. Use the UUCG loop as a fingerprint reference (if present).
3. Perform this comparison every time before ^1H $R_{1\rho}$ RD experiments are recorded.

3. ^1H $R_{1\rho}$ Relaxation dispersion— on-resonance (labeled 1D version)

NOTE: The steps below describe the setup of RD experiments for a labeled sample using the 1D version of the HSQC-based RD pulse sequence. Follow the same steps for the SELOPE-based 1D sequence for unlabeled samples. An overview of parameter names and settings for both cases are shown in **Table 2**. The focus on 1D versions is because they are more practical for off-resonance measurements, and the setup of the 2D versions of the SELOPE and HSQC-based experiments have been discussed in detail by Schlagnitweit et al.²⁰ and Steiner et al.¹⁰, respectively.

1. Determine ^1H power for a **hard 90°** pulse (P1).
 1. Option A: Use Bruker **pulsecal** command.
 2. Option B: In a **zg** experiment, determine the 360° pulse by measuring a nutation curve at the proton hard-pulse power level on the water peak.

NOTE: The 90° pulse length is a fourth of the duration where zero signal is observed (if a full nutation curve is measured, then it is the second zero; however, in practice, only the region around the expected value for the 360° is sampled).
2. Run a ^1H 1D spectrum **zgesgp.f2f3dec** using the pulse length determined in step 3.1 to confirm the RNA folding before every $R_{1\rho}$ measurement.

NOTE: If ^1H SL experiments are run for the first time, check if the calculated SL power corresponds to the power delivered to the sample by calibrating SL power for each desired bandwidth. Detailed calibration steps are described in Steiner et al.¹⁰.

3. Create a ^1H $R_{1\rho}$ for labeled data set, and set key parameters.
 1. Create a new data set; ideally based on a ^1H - ^{13}C aromatic HSQC data set as used on fully labeled RNA samples for RNA assignment.

NOTE: This will ensure that ^{13}C as well as ^{15}N power and decoupling power are already set up.
 2. Set the general parameters according to the first part of **Table 2**.
 3. Set RD-specific parameters according to the second part of **Table 2**.
 4. Set ^1H SL power to the lowest value (1.2 kHz) for testing.
 5. Generate a **test vd list** with only one entry, **0 ms**, (to optimize the vd list, as described in step 3.4), set **TDF1** to 1, and update **D30**.
 6. Run a test spectrum with these settings.
4. Optimize the vd list (list of SL lengths to be used).
 1. Run the experiment with a **test** vd list (e.g., six entries: 0 m, 5 m, 10 m, 20 m, 30 m, 40 m; scramble these values to avoid systematic errors due to heating).
 2. Update **D30** and **TDF1** accordingly (in this example, D30 = 42m and TDF1 = 6).

- Plot intensity of the peak vs. SL length. Identify the SL length at which the intensity of the original peak decreases to 1/3.
- Create the final vd list to be used in the experiment, taking into consideration the following: determine the longest SL length as described in the previous step; avoid using a list with decreasing or ascending order; and add some duplicates for statistical studies. Remember to update D30 and TDF1 every time there are any changes in the vd list.

NOTE: The experiment is run with different SL lengths as given in the vd list in a pseudo-2D way.

- Select the number of scans so that the weakest peak of the list has a signal-to-noise ratio (SINO) of at least 10.

NOTE: Although the vd list was optimized for a low SL power (1.2 kHz), this vd list should also be tested at the highest SL power to be used (e.g., 15 kHz). This is because the decay will be much slower at high SL power for peaks with significant k_{EX} contribution. Therefore, a sufficient decay should also be verified at high SL power.

Parameter Description	Parameter name in pulse sequence	
	1D labeled	1D SELOPE
pulse program for on-resonance 1Ds	1HR1rho_HCP_onres1D.es	1HR1r_HH_onres1D.js
^1H carrier frequencies (ppm)	O1P = water resonance in ppm	O1P = chemical shift of peak of interest (ppm)
	CNST28 = chemical shift of peak of interest (ppm)	CNST29 = water resonance in ppm
^1H hard 90° pulse	P1 @ PL1 (as calibrated in 3.1.1)	P1 @ PL1 (as calibrated in 3.1.1)
Shaped pulses and powers for water suppression	P25 = 1000 us @ sp3	P12 = 2000 us @ sp1
	(Watergate)	(excitation sculpting)
^{13}C carrier frequency, on-resonance with ^{13}C chemical shift of peak of interest	O2P	–
^{15}N carrier frequency, average ^{15}N chemical shift for decoupling (as used in aromatic HSQC)	O3P	–
$^{13}\text{C}/^{15}\text{N}$ decoupling (set up as in HSQC)	pcpd2, cpd2	–
	pcpd3, cpd3	–

HCP transfer (e.g., $p=1/J$ @ 100 Hz)		–
pulse and pulsef2 commands can be used to determine powers from hard pulses		
Duration (set to $1/J(^1\text{H}-^{13}\text{C})$ of peak of interest)	P11	
Power ^1H and Power on ^{13}C	SP1, SP12	
SELOPE transfer ($d = 1/4J(\text{H5}-\text{H6})$)	–	D5
Selective pulse (e.g., aromatic region) for SELOPE (4000 us, Eburp)	–	P13 & SP4
SL / RD-specific parameters:		
^1H SL power, obtained from calibrated hard pulse (e.g., using the pulse command).	PI25 & CNST12 (1.2 – 15 kHz)	PI24 (50 Hz – 15 kHz)
Variable delay list for SL duration (initially 1 entry, 0, optimization described under 3.1.3)	vdlist (~ 0 – 40 ms)	vdlist (~ 0 – 150 ms due to the low R_2 in unlabeled samples)
TDF1 number of entries in the vd list (initially 1)	TDF1	TDF1
Heat compensation:		
D30 = largest value in vd list + 2ms	D30	D30
Additional heat compensation for very broad range of SLs		PL25
Off-resonance specific parameters:		
pulse program for off-resonance 1Ds	1HR1rho_HCP_offres1D.es	1HR1r_HH_offres1D.js
Offset for off-resonance experiments	CNST30	CNST30

Table 2: Overview of parameters to set up 1D HCP-based and 1D-SELOPE-based ^1H $R_{1\rho}$ experiments. Abbreviations: 1D = one-dimensional; HCP = heteronuclear cross-polarization; SELOPE = SElective Optimized Proton Experiment; ppm = parts per million; HSQC= heteronuclear spin quantum correlation; SL = spin lock; RD = relaxation dispersion

5. Set-up and acquisition of on-resonance ^1H $R_{1\rho}$ experiments

1. Copy the experiment from section 3.4 into a new folder in **Topspin**.
2. In this folder, set up experiments at different SL strengths, each time changing **PL25** and **CNST12**. Determine the correct power level for each SL strength by using the **pulse** command. Use SL strengths ranging from 1.2 to 15 kHz, with a denser sampling for lower SL strengths (see **Figure 5G** for selected SL strengths). Add copies of some of the experiments to have duplicates for some of the SL strengths.
3. Run these experiments.

6. Analysis of on-resonance ^1H $R_{1\rho}$ experiments

1. In TopSpin, process each slice of each pseudo-2D data set using the same processing parameters (e.g., line broadening, phase) using the command **xf2**, and split the dataset into 1Ds using the Bruker AU program **split2D**.

2. Obtain signal intensities and volumes for each 1D slice.

NOTE: In practice, it is better to deconvolve the spectra to get rid of contributions from potentially overlapping peaks and allows the usage of the Bruker AU program **multidcon**, which conveniently summarizes the intensities or areas of the peaks of all slices in one experiment in the text file **decall.txt**, which can then be read out easily with other programs (Python scripts written in-house were used here, as described by Steiner et al.¹⁰) in steps 3.6.3 and 3.6.4.

3. Fit a mono exponential decay for each SL strength to obtain the $R_{1\rho}$ (or on-resonance, R_2+R_{EX}) value.

4. Plot those R_2+R_{EX} values (y) vs. SL strength (x) (**Figure 5F,G**).

NOTE: If the values are significantly higher for low SL strengths and decrease with higher SL power (as shown in **Figure 5G**), then the investigated peak shows dispersion, and it might be interesting to carry out additional (off-resonance) experiments to obtain information about the population and chemical shift difference of the excited state vs. the ground state.

4. ^1H $R_{1\rho}$ Relaxation dispersion—off-resonance (labeled 1D version)

1. Set-up and acquisition of off-resonance ^1H $R_{1\rho}$ experiments

1. In a new topspin folder, set up experiments at a certain SL strength (usually first at the lowest SL strength as the R_{EX} contribution is highest there, see **Figure 5G** for a representative selection of off-resonance SLs), but with different offsets, each time changing **CNST30**.

2. Use offsets up to $\pm (3 \text{ or } 4) \times \text{SL strength}$, with a denser sampling around 0 offset, as can be seen in **Figure 5H,I**.

3. Run these experiments.

2. Analysis of off-resonance ^1H $R_{1\rho}$ experiments

1. Use the same processing strategy, as in 3.6.1–3.6.3, to determine an $R_{1\rho}$ value for each offset.

2. Plot those values vs. offset (**Figure 5G**).

NOTE: An asymmetry in this curve can already indicate that chemical shift information for the excited state can be obtained. Thorough fitting and analysis using Bloch-McConnell or Laguerre equations have to be carried out to obtain information on k_{EX} , ρ_{ES} as well as $\Delta\omega^{10,20}$ (**Figure 5G**). Example datasets, pulse programs, and macros for both 1D experiments can be found on the Petzold Lab Github repository (<https://github.com/PetzoldLab>). An overview of parameters is given in **Table 2**.

Representative Results

The protocol for RNA production facilitates purification through the generation of high-purity transcripts. **Figure 3A** shows the results of several cleavage reactions of tandem transcripts, providing both successful and unsuccessful reactions. Lane 1 shows the optimal case of a fully cleaved transcript with only faint traces of side products. Lane 2a shows incomplete cleavage, which can be resolved by re-annealing and the addition of more RNase H (Lane 2b, step 2.1.2). The RNA constructs of lanes 1, 2a, and 2b are the same. The sample in lane 3 shows unsuccessful cleavage. Troubleshooting this reaction would involve a check of the cleavage guide sequence, purity of DNA template, and annealing temperatures. Potentially, RNase H cleavage will have to be performed after T7 IVT as shown for sample 2.

The sample in lane 4 shows a significant amount of cleavage side products, which are difficult to remove via ion-exchange HPLC. Troubleshooting such a sample can involve (a) lowering temperature, amount of RNase H, or reaction time, (b) reducing elution gradient and injection volume and attempting to separate the target fractions from the side products. Further information on how to increase

the resolution in ion exchange HPLC purification has been discussed by Karlsson et al.³¹. HPLC separates the target RNA from longer or shorter nucleic acids and protein or small-molecule contaminants. **Figure 3B** shows the optimal result for the ion-exchange HPLC purification. The elution gradient should be chosen such that the target RNA species elutes at least one column volume (in this example: 35 mL) after the next smaller species and one column volume before the next larger species.

Smaller species in this method include single nucleotides, abortive products (8-12 nt), 3' and 5' spacer sequences (5-14 nt), and cleavage guide (12 nt chimeric nucleic acid), whereas longer sequences are potentially uncleaved tandem repeats and the plasmid. When a well-separated elution peak is achieved, purification can be scaled up to the equivalent of ~20 mL of IVT reaction per injection. The correct fold of an RNA sample is crucial for RD experiments and has to be confirmed before every measurement. **Figure 4** shows an A-labeled 22-mer RNA before the folding protocol in step 2.4 (blue) was applied, and the same sample after the correct folding has been achieved (red). A Mc-Fold secondary structure prediction (**Figure 4C**) proposes the presented hairpin structure with 4 base pairs resulting in 5 imino signals.

Both spectra in **Figure 4A** confirm these predicted signals, albeit with slightly different relative intensities, which indicates that some misfolded structure (here, a dimer) can be problematic to assess with only ^1H 1D spectra. An aromatic ^1H , ^{13}C -HSQC spectrum (**Figure 4B**), however, shows only 3 of the aromatic signals for the sample before the folding protocol (blue), but all 4 signals for the sample that has been folded according to step 2.4 (red). The sample shown in blue likely formed a homodimer (structure proposed in **Figure 4D**) that would result in the same imino signals

as the hairpin. The signal of A13H2 seems exchange-broadened. These results help to highlight the importance of folding confirmation with both imino and aromatic fingerprint experiments before each RD experiment. The ^1H $R_{1\rho}$ pulse sequences described in this protocol allow the detection of dynamics in the intermediate exchange regime. Initially an on-resonance curve is recorded, and if dynamics are present for a specific residue, a dispersion is visible within the obtained R_2+R_{EX} values, while this curve is flat for residues without exchange.

Figure 5 shows representative on-resonance curves obtained for two different H8 atoms in a synthetic RNA hairpin (**Figure 5A**), wherein G6H8 experiences exchange (**Figure 5C**), while A4H8 does not (**Figure 5B**). As the exchange is relatively slow in this sample ($k_{EX} = 292 \pm 40$ Hz), the advantage of the SELOPE experiment to achieve low SL strengths was exploited, and the two on-resonance curves were recorded using the 1D version of the pulse sequence. The same pulse sequence was then used to obtain off-resonance data for the residue showing dispersion in the on-resonance profile. **Figure 5D** shows the obtained $R_{1\rho}$ values vs. offset wherein a slight asymmetry of the curve already indicates the sign of $\Delta\omega$.

This becomes even more apparent in the R_2+R_{EX} plot where the R_1 contribution is removed (**Figure 5E**). The right column of the same figure shows representative on-resonance curves obtained for two different H8 atoms in a slightly different synthetic RNA hairpin with faster exchange, wherein G6H8 experiences exchange (**Figure 5G**), whereas A4H8 does not (**Figure 5F**). The faster exchange rate ($k_{EX} = 43,502 \pm 38,478$ Hz) allowed the RD recording of all aromatic protons at once using the SELOPE 2D version to obtain both, on- and off-resonance data (G6H8 data displayed in **Figure 5H,I**).

General identifiers for positive and negative results

Positive results in the tandem IVT and RNase H cleavage can be identified as follows: 1) The target band is the strongest band in the denaturing PAGE gel. 2) There are no or only weak bands around the main band. 3) There are no or only weak higher molecular weight species. 4) The HPLC chromatogram shows a well separated peak of the target RNA. 5) When the main peak is sampled, only one band appears on a denaturing PAGE gel.

Negative results in the tandem IVT and RNase H cleavage present as follows: 1) No or just a weak main band is visible on a denaturing PAGE gel. 2) A pattern of high molecular weight species from RNA tandem repeats is visible. 3) Although the main band is present, bands of similar intensity are above or below the main band within ± 3 nt.

A well-folded sample can be identified as follows: 1) The number of observed imino protons matches the number of imino protons expected from a secondary structure simulation (e.g., Mc-Fold³⁹, **Figure 4A**). 2) The syn G-U wobble base pair in a UUCG loop (if present) is visible at ~ 9.5 ppm, sometimes only visible at lower temperature. Further fingerprinting of the UUCG loop has been described by Fürtig and colleagues⁴⁰. 3) The aromatic fingerprint agrees with a previously assigned sample that has been confirmed to fold correctly (**Figure 4C**).

A misfolded or degraded sample can be identified as follows: 1) There are more imino signals than a secondary structure simulation predicts (**NOTE**: fewer imino signals do not necessarily imply misfolding, as closing base pairs are often not visible, and conformational exchange broadens lines). 2) Absence of imino signals. 3) Narrow signals of high intensity in the aromatic region, indicating single nucleotide degradation products. 4) Divergence between

imino or aromatic signals to a reference sample of confirmed folding (**Figure 4C**).

An atom showing no exchange in the detectable timescale can be identified as follows: 1) from a flat RD profile (due to the missing R_{EX} contribution varying with the applied SL power) (**Figure 5B** and **Figure 5F**). 2) Care has to be taken for the case of slow-intermediate exchange when k_{EX} and $\Delta\omega$ are of the same magnitude. In that case, the on-resonance contribution can be very small as can be seen in **Figure 5C** (in this case the fitted parameters are $k_{EX} = 292 \pm 40$ Hz and $\Delta\omega = 112 \pm 4$ Hz). If in doubt, a low SL off-resonance curve can be recorded for verification.

An atom showing exchange in the intermediate time scale can be identified 1) from a non-flat relaxation dispersion profile in an on-resonance RD experiment (**Figure 5B** and **Figure 5F**); 2) a broader linewidth in the HSQC or SELOPE experiment can also be an indicator for exchange.

Well-selected SL power values for off-resonance curves (**Figure 5E,F**): 1) have a considerable k_{EX} contribution in the on-resonance curve (selected SL power values are indicated in **Figure 5C** and **Figure 5G**). 2) As off-resonance curves are measured for at least 3 SL power values, the selected SL power values should be spread out over the region of the on-resonance curve with k_{EX} contribution. 3) Lead to non-flat $R_2 + R_{EX}$ curves after the Laguerre fit (e.g., **Figure 5D**: SL strengths 25, 50, and 75 Hz; **Figure 5E**).

Poorly selected SL power values for off-resonance curves (**Figure 5E,F**) lead to flat $R_2 + R_{EX}$ curves after the Laguerre

fit. An example is shown in **Figure 5E**, wherein the 100 Hz off-resonance curve is very flat and therefore does not provide significant information on $\Delta\omega$.

Indications for rotating-frame nuclear Overhauser effect (ROE) artefacts: 1) $\Delta\omega$ obtained from off resonance curves match chemical shifts of protons in spatial vicinity / protons, which show a cross peak with the peak of interest in the nuclear Overhauser effect spectroscopy (NOESY) spectrum. (e.g., **Figure 5I** shows broad off-resonance curves as expected for fast-intermediate exchange, but the curves also have sharper features, e.g., at -3000 Hz and +1500 Hz. These are very likely due to an ROE artifact rather than a chemical shift for this H8 in a different conformer). 2) Laguerre fit does work, but does not work well (gives high errors or physically impossible values) for an on-resonance and at least 3 off-resonance curves, even though exponentials were obtained from experiments with high SINO (>20) (e.g., $k_{EX} = 43,502 \pm 38,478$ Hz). Often each SL fits individually well, but fitting them together gives a much higher error; the opposite behavior is expected for a true excited state.

Indications for “true” exchange $\Delta\omega$: 1) $\Delta\omega$ obtained from off-resonance curves do not match chemical shifts of protons in spatial vicinity/protons, which show a cross peak with the peak of interest in the NOESY spectrum (e.g., **Figure 5E**). 2) Laguerre fit gives low errors for an on-resonance and at least 3 off-resonance curves (e.g., **Figure 5E** vs. **Figure 5I**, see caption for fit results).

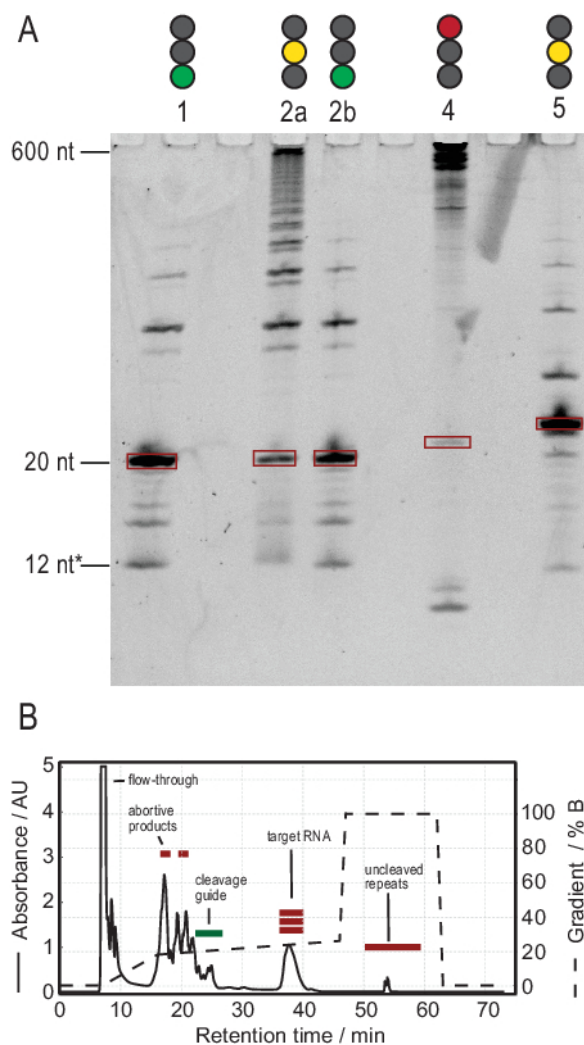


Figure 3: Sample production by T7 tandem IVT and RNase H cleavage reaction. (A) Denaturing PAGE of positive and negative results of tandem IVT and RNase H cleavage. Ladder height refers to RNA references, 12* refers to the chimeric cleavage guide. Lane 1: Successful generation of a 20 nt target RNA. Few shorter and longer products are present. Lane 2a: Incomplete cleavage of the tandem transcript. Although HPLC purification is possible, a lot of material would be wasted. Lane 2b: Continued RNase H cleavage of Lane 2 produces a clean sample ready for HPLC injection (identical to Lane 1). Lane 4: RNase H cleavage was largely unsuccessful, and no target band was produced. The full-length tandem transcript is still visible at 600 nt. Lane 5: A target band was produced, but a strong -1 band is present. Although HPLC can be performed, careful removal of the side product is necessary. **(B)** Example of a successful HPLC injection. The peak at 38 min contains pure RNA of the target length, while longer and shorter products are well-separated from the target RNA. Panel B has been modified from ²¹. Abbreviations: IVT = *in vitro* transcription; HPLC = high-performance liquid chromatography; nt = nucleotides; AU = arbitrary units. [Please click here to view a larger version of this figure.](#)

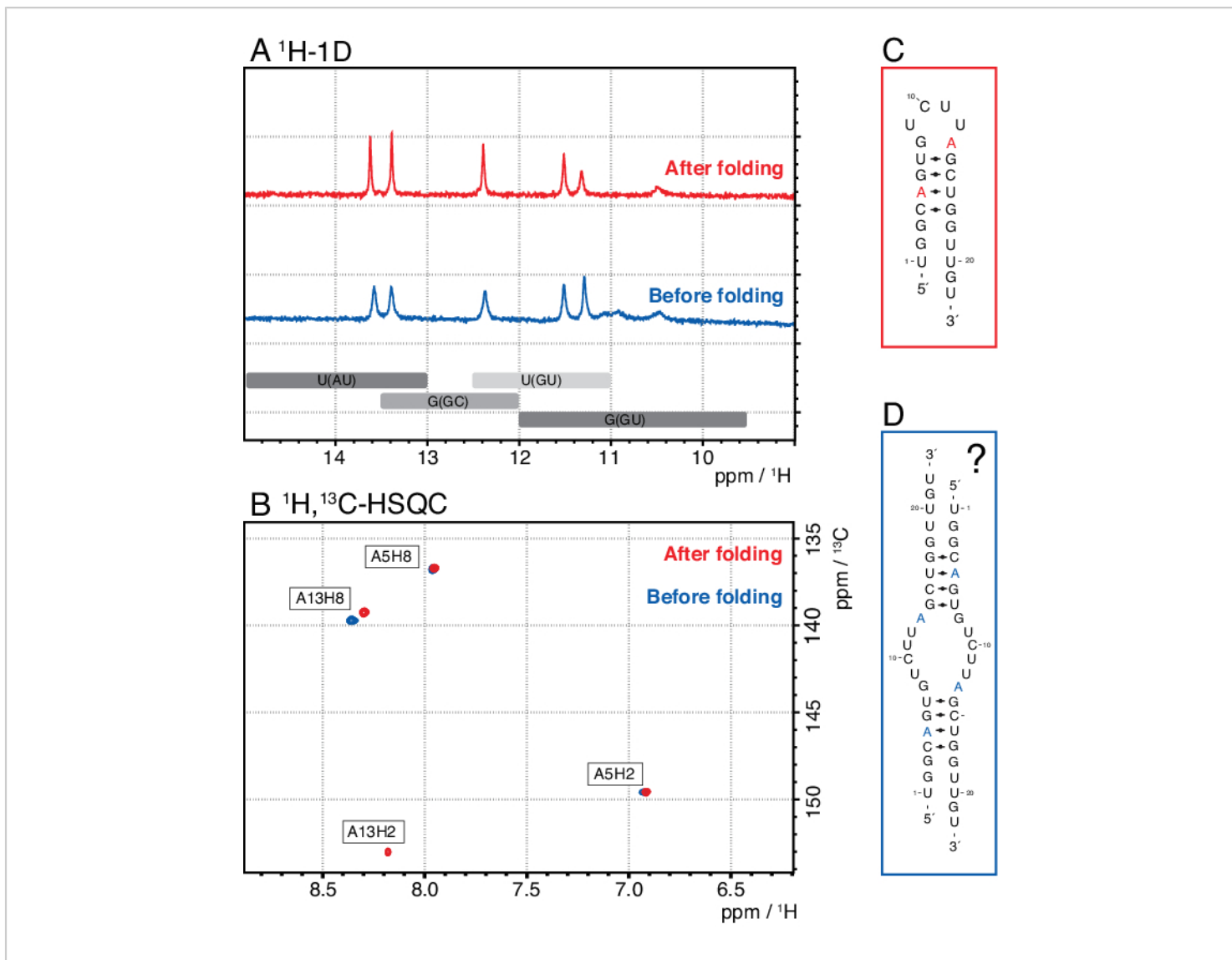


Figure 4: Example of an RNA hairpin before (blue) and after (red) the folding step 2.4 (see protocol) in NMR. (A) Imino region of a ^1H -1D spectrum of an A-labeled 22-mer RNA. Expected regions for base pair identity of imino signals are indicated in gray below. **(B)** ^1H , ^{13}C -HSQC spectrum of the aromatic resonances of the RNA from panel A. The sample after folding (red) shows 4 signals as expected, while the sample before folding (blue) shows only 3 signals. **(C)** Mc-Fold prediction of the 22-mer RNA as a hairpin. Five imino signals are to be expected from this secondary structure, which can be found in both samples in panel A. **(D)** Proposed structure of a homodimer formed by the 22-mer RNA, resulting in the same 5 base pairs as the hairpin structure. Abbreviations: NMR = nuclear magnetic resonance; 1D = one-dimensional; HSQC = heteronuclear single quantum correlation; ppm = parts per million. [Please click here to view a larger version of this figure.](#)

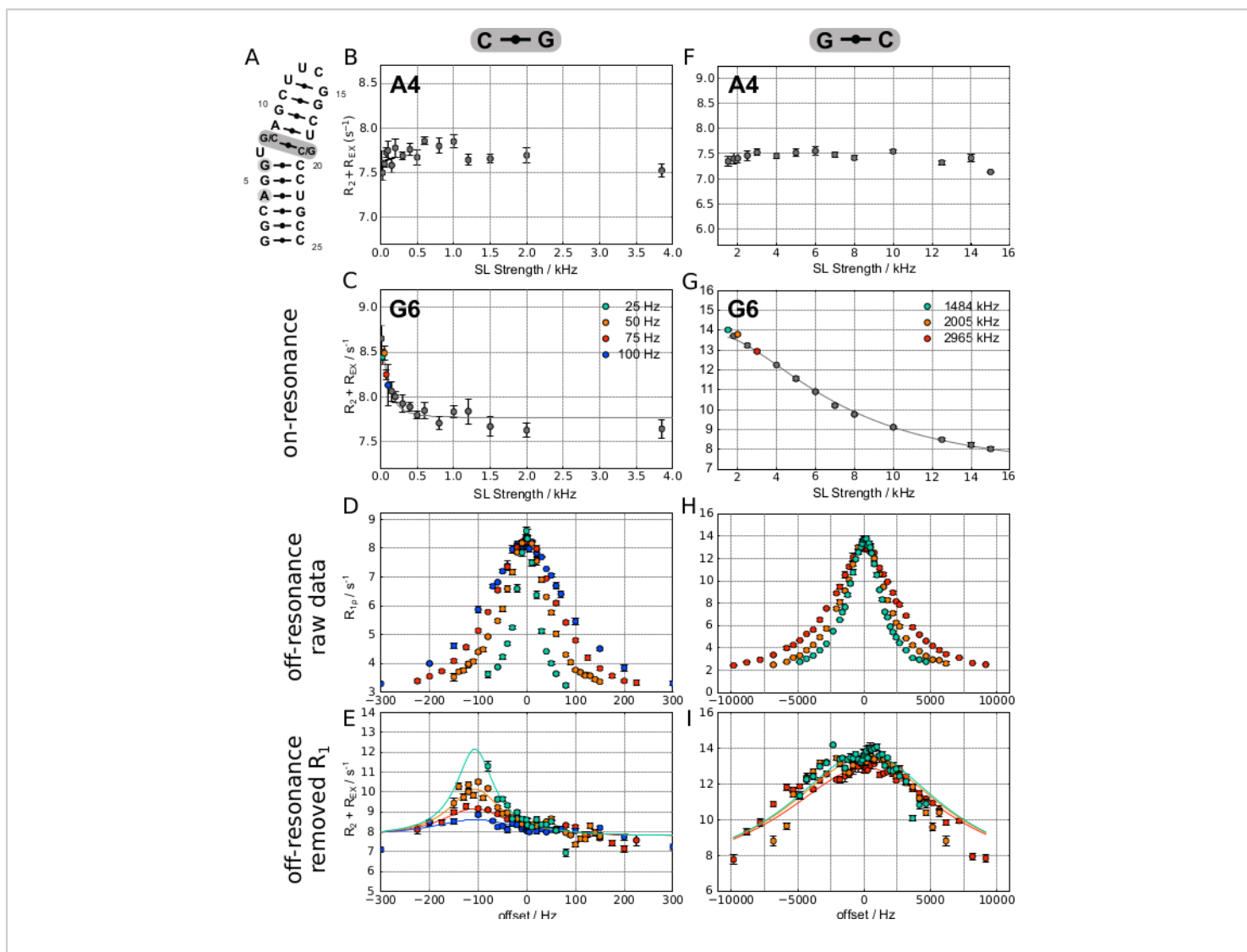


Figure 5: ^1H $R_{1\rho}$ RD representative results for two different constructs based on an RNA hairpin. (A) The left column shows results obtained on the RNA with a C-G base pair above the bulged U, while the right column shows results obtained on a sample where the base pair was switched to G-C instead. (B) and (F) show flat dispersion profiles as obtained for A4H8 for the two constructs, indicating no conformational exchange. (C–E) show on-resonance, off-resonance, and fitted data obtained for G6 in the (G-C) construct. The Laguerre fit leads to the following result: $R_1 = 2.87 \pm 0.01$ Hz, $R_2 = 7.76 \pm 0.03$ Hz, $k_{EX} = 292 \pm 40$ Hz, $p_{ES} = 0.31 \pm 0.03$ %, $\Delta\omega = 112 \pm 4$ Hz. (G–I) show on-resonance, off-resonance, and fitted data obtained for G6 in the (G-C) construct. The Laguerre fit leads to the following result: $R_1 = 1.93 \pm 0.02$ Hz, $R_2 = 6.71 \pm 0.86$ Hz, $k_{EX} = 43,502 \pm 38,478$ Hz, $p_{ES} = 27 \pm 16$ %, $\Delta\omega = 203 \pm 166$ Hz. This figure was modified from ²⁰. Abbreviation: SL = spin lock. [Please click here to view a larger version of this figure.](#)

Discussion

The protocol presented herein is a synthesis of several protocols published previously in the form of research articles^{10,20,21,31}. Hence, segments of the protocol can be applied, while others can be exchanged to the preference of the reader. For example, the $R_{1\rho}$ measurements can be performed on an RNA sample produced with any method, given that folding and homogeneity of length are assumed. Furthermore, the protocol does not contain information on resonance assignment of the RNA sequence—a step required for RD experiments—as this has been covered extensively in previous literature^{19,37,38}. Partial, segmental, or site-specific labeling schemes^{36,41,42,43,44} are approaches to facilitate resonance assignment or reduce the overlap of resonances that are of interest in RD experiments and have been described at length in the literature. This method allows the use of uniform labeling of any nucleotide identity, which can already simplify resonance assignment significantly.

The IVT method presented here overcomes known issues with sequences and labeling, increases yield, and decreases cost and work time compared to other methods. The use of the viral initiation sequence reduces the need for reaction optimization, which is a known problem in the field that can be time-consuming to perform and yields only few copies of the transcript in the case of non-G initiation. The T7 IVT and RNase H cleavage of the tandem transcript can be performed simultaneously in the same vessel. A pattern of multimeric tandem repeats can be seen on a denaturing PAGE gel during the reaction, which coalesces to a single band on the target RNA upon completion of RNase H reaction (**Figure 3A**, lanes 1 and 2b). Typical yields using this method range between 30 and 70 nmol RNA per 1 mL IVT. Yet, the method based on RNase H cleavage of tandem repeats does not come without certain problems of its own. The RNase H cleavage reaction

often does not go to completion when run simultaneously with T7 transcription (**Figure 3A**, lane 2a).

The separation of tandem units can be finalized by annealing the cleavage guide to the transcript and adding more RNase H (**Figure 3A**, lane 2b, step 2.1.2). As heating of large volumes is slow and leads to Mg^{2+} -catalyzed hydrolysis of RNA, a conventional microwave oven was used, which heats the sample to >95 °C in 10-15 s. Adverse effects on the produced samples have not been observed so far. Some constructs show a minor second band that could not be eliminated by the optimization of the reaction conditions (**Figure 3A**, lane 4). Usually these are rather clearly visible as a shoulder in the HPLC chromatogram, if a well-optimized elution gradient is used, and can be removed (step 2.2.5). The following discussion is aimed to highlight critical steps in the protocol, specifically with respect to obtaining high-quality data that allow an interpretation of conformational dynamics.

RNase contamination

Extracellular RNases are ubiquitous, highly stable, and pose the biggest threat for long-term stability of NMR samples. Therefore, it is crucial to work in an RNase-free environment and keep all reagents and plasticware RNase-free. The use of filter tips and maybe even facemasks is recommended. This is specifically important after HPLC purification. NMR samples contaminated with RNases typically exhibit narrow peaks visible in 1H -1D spectra after days or weeks due to single-nucleotide degradation products. Such a sample is not suitable for $R_{1\rho}$ measurements.

NMR sample

Owing to its highly charged nature, RNA can be used in high concentrations without precipitation when compared to most proteins. The use of Shigemi NMR tubes (see the **Table of Materials**) is advantageous as they allow centering of the

highly concentrated sample in the center of the coil while still providing ideal shimming and locking conditions due to the susceptibility-matched glass bottom and plunger. This way, B1-inhomogeneity is reduced, giving rise to narrower lines. The typical sample volume in an NMR tube is 250 μL , and typical concentration is 1-2 mM. Samples below 500 μM are not recommended for RD experiments as the experiment would take too long and a good shim. Similarly, sample volume below 200 μL is not recommended because a good shim and field stability (lock) is required. When inserting the plunger, it is crucial to avoid the formation of bubbles in the sample (step 2.4.5). If not fixed properly, the plunger can slide down into the sample, reducing the detectable volume. Furthermore, rapid changes in temperature can lead to the formation of new bubbles in the sample. Therefore, care should be taken when transporting the sample and when changing the probe temperature in the NMR spectrometer. Check the sample for bubbles when measuring again after a longer period.

RNA folding

Dynamic RNA molecules can exist in multiple conformations when not folded properly. Even though melting temperatures of secondary structures can be only slightly above room temperature, a thorough heating-and-snap-cooling procedure is recommended before measurement. Highly concentrated hairpin samples folding under kinetic control (heating-and-snap-cooling) can form homodimers over time, which necessitates rigorous control of RNA folding before each NMR measurement. If the measured RNA is not a hairpin structure but an RNA duplex, slow folding under thermodynamic control should be applied.

In this case, the cooling process after heating should be in the range of hours, while the RNA is used at its final volume and

concentration in the NMR sample. An initial count of expected imino and aromatic resonances can provide insight about the homogeneity of the sample. If the sample does not look like expected, it should be re-folded. Mg^{2+} (added as chloride salt) can help with folding RNA structures⁴⁵. In practice, the folding control serves as a comparison to a sample that has been used to at least partially assign the NMR resonances and to solve the secondary structure experimentally.

Spin lock power and heating considerations

In case of running the ^1H $R_{1\rho}$ RD experiments as 2D overview experiments, SL power should be no lower than 1.2 kHz. The radiofrequency transmitter frequency should be placed in the middle of the ppm region of the peaks of interest (e.g., 7.5 ppm for aromatic protons). The bandwidth of 1.2 kHz will then be large enough to spin-lock these protons without any major off-resonance effects. Such effects can be identified in the RD profile. If they occur, $R_{2+R_{EX}}$ values increase instead of decrease with increasing SL power values, especially for low SL power. Check if the calculated SL power values correspond to the power delivered to the sample. In practice, calculated SL power can be used if the ^1H 90° hard pulse was calibrated carefully on newer spectrometers; however, this can be checked by calibrating SL power for each desired bandwidth.

The range of SL power, which can be used in ^1H $R_{1\rho}$ RD experiments is very broad, leading to varying sample heating (1.2 kHz to 15 kHz for HSQC for HCP-based sequences and 50 Hz to 15 kHz for SELOPE experiments). Unequal sample heating can be detected as a slight change in chemical shift when comparing 1Ds obtained for low power SLs vs. high power SLs. This effect is usually not considered in heat compensations in $R_{1\rho}$ experiments on heteronuclei. Heat compensation in those experiments is usually set up

to correct for different heating due to the different spin lock durations specified in the vd list of each spin lock power series. Especially for the SELOPE experiment, a second heat compensation should be used across all applied SL strengths as described in²⁰.

vd list considerations

As mentioned earlier, the vd list should contain a time point long enough to obtain a significant decay of intensity (ideally down to 30% of initial signal, or as low as possible if it is not possible to reach a 70% decay within the specifications of the probe). Although the vd list was optimized for a low SL power (1.2 kHz), this vd list should also be tested at the highest SL power to be used (e.g., 15 kHz). This is due to the fact, that for peaks with significant R_{EX} contribution, the decay will be much slower at high SL power. So a sufficient decay should also be verified at high SL power. The same must be considered for decays at high offsets in off-resonance experiments. The ideal maximum time point of the vd list could be significantly different for the different regions of the dispersion experiment. In that case, more points could be included in the vd list, and the longer vd list points for higher SL power or higher offsets during analysis, based on the low SINO they will lead to, could be discarded. In general, 5-8 vd list points should be considered to be able to spot potential artefacts leading to non-exponential decays such as J-coupling (see below).

1D-HCP selectivity considerations

Special care must be taken when running the HCP-based 1D version if there is another peak overlapping with the peak of interest in the ^1H dimension of the 2D HSQC-based experiment. HCP-based transfers are very, but never 100% selective, and it can therefore happen that another peak contributes to the intensity and decay behavior of the peak of

interest in the 1D. An indication for this would be a difference in on-resonance $R_{1\rho}$ values obtained using the 1D and 2D versions of the labeled experiment.

ROE considerations:

For off-resonance curves of atoms with slow-intermediate exchange, ROE artefacts can be identified based on a comparison of the obtained $\Delta\omega$ with a NOESY or ROESY spectrum. If a cross peak can be identified at a chemical shift difference corresponding to $\Delta\omega$, then the observed excited state might in fact be a ROE artifact (e.g., ROEs were found between aromatic protons, which are all in the same chemical shift range and therefore covered by those off-resonance curves²⁰). From experience, this always also led to poor fits with large errors, possibly due to the ROE not following the same pattern as R_{EX} with increasing SL power. The situation becomes more difficult for intermediate-fast exchange. While the on-resonance curve is (from comparison with ^{13}C data obtained on the neighboring nucleus) still representative of the exchange process between the GS and ES, the off-resonance curve is influenced by multiple ROE artefacts.

In that case, the SL power to detect the exchange process is larger (>1.5 kHz) and therefore spans a larger number of protons as off-resonance curves span over chemical shift differences of various ROE candidates (for H8 these would be: amino protons at ca. ± 1000 Hz, H5/H1's at ca. -1200 Hz, imino protons at ca. 3500 Hz). So far, no method has been found to suppress these ROE artefacts (other than using partially deuterated nucleotides⁴⁶), and off-resonance data should not be recorded for fast-intermediate exchange, as no reliable information on the actual $\Delta\omega$ can be extracted with this method, if NOE/ROE contribution cannot be excluded via NOESY spectra.

J-Coupling (Hartmann-Hahn) considerations

Although on-resonance curves for homonuclear J-coupled protons, such as H6, were successfully recorded^{10,20}, special care must be taken for off-resonance measurements, especially for low SL power as Hartmann-Hahn matching conditions can span a wide range of the investigated offsets. Hartmann-Hahn artefacts can be identified as oscillations on the exponential decay or increasing R_2+R_{EX} values with increasing SL strengths in on-resonance RD plots²⁰.

Skłodowska-Curie IF (EU H2020, MSCA-IF project no. 747446).

Disclosures

K.P. is consultant to Arrakis Therapeutics, a company that discovers small molecules targeting RNA.

Acknowledgments

We thank the protein science facility (PSF) at the Karolinska Institutet for expression and purification of T7 RNA polymerase and *E. coli* RNase H, Martin Hällberg for the generous gift of the inorganic phosphatase, and the entire Petzoldlab for valuable discussions. We thank Luca Retattino for preparation of the U-bulge constructs and Emilie Steiner and Carolina Fontana for their contribution to macros and fitting scripts. We acknowledge the Karolinska Institute and the Dept. of Medical Biochemistry and Biophysics for the support of the purchase of a 600 MHz spectrometer and position financing (KI FoAss and KID 2-3707/2013). We are grateful for financial contribution from Vetenskapsrådet (#2014-4303), Stiftelsen för strategisk Forskning (ICA14-0023 and FFL15-0178) and The Ragnar Söderberg Stiftelse (M91-14), Harald och Greta Jeansson Stiftelse (JS20140009), Carl Tryggers stiftelse (CTS14-383 and 15-383), Eva och Oscar Ahréns Stiftelse, Åke Wiberg Stiftelse (467080968 and M14-0109), Cancerfonden (CAN 2015/388), J.S. acknowledges funding through a Marie

References

1. Djebali, S. et al. Landscape of transcription in human cells. *Nature*. **489** (7414), 101-108 (2012).
2. Doudna, J. A., Cech, T. R. The chemical repertoire of natural ribozymes. *Nature*. **418** (6894), 222-228 (2002).
3. Sehgal, P. B., Westley, J., Lerea, K. M., DiSenso-Browne, S., Etlinger, J. D. Biomolecular condensates in cell biology and virology: phase-separated membraneless organelles (MLOs). *Analytical Biochemistry*. **597**, 113691 (2020).
4. Herschlag, D., Allred, B. E., Gowrishankar, S. From static to dynamic: the need for structural ensembles and a predictive model of RNA folding and function. *Current Opinion Structural Biology*. **30**, 125-133 (2015).
5. Kimsey, I. J., Petzold, K., Sathyamoorthy, B., Stein, Z. W., Al-Hashimi, H. M. Visualizing transient Watson–Crick-like mispairs in DNA and RNA duplexes. *Nature*. **519** (7543), 315-320 (2015).
6. Dethoff, E. A., Petzold, K., Chugh, J., Casiano-Negrone, A., Al-Hashimi, H. M. Visualizing transient low-populated structures of RNA. *Nature*. **491** (7426), 724-728 (2012).
7. Baisden, J. T., Boyer, J. A., Zhao, B., Hammond, S. M., Zhang, Q. Visualizing a protonated RNA state that modulates microRNA-21 maturation. *Nature Chemical Biology*. **17** (1), 80-88 (2021).
8. Marušič, M., Schlagnitweit, J., Petzold, K. RNA dynamics by NMR spectroscopy. *Chembiochem*. **20** (21), 2685-2710 (2019).
9. Baronti, L. et al. Base-pair conformational switch modulates miR-34a targeting of Sirt1 mRNA. *Nature*. **583** (7814), 139-144 (2020).
10. Steiner, E., Schlagnitweit, J., Lundström, P., Petzold, K. Capturing excited states in the fast-intermediate exchange limit in biological systems using ¹H NMR spectroscopy. *Angewandte Chemie International Edition*. **55** (51), 15869-15872 (2016).
11. Moschen, T. et al. Ligand-detected relaxation dispersion NMR spectroscopy: dynamics of preQ1–RNA binding. *Angewandte Chemie International Edition*. **54** (2), 560-563 (2015).
12. LeBlanc, R. M., Longhini, A. P., Tugarinov, V., Dayie, T. K. NMR probing of invisible excited states using selectively labeled RNAs. *Journal of Biomolecular NMR*. **71** (3), 165-172 (2018).
13. Strebiter, E., Nußbaumer, F., Kremser, J., Tollinger, M., Kreutz, C. Studying sparsely populated conformational states in RNA combining chemical synthesis and solution NMR spectroscopy. *Methods*. **148**, 39-47 (2018).
14. Rangadurai, A., Shi, H., Al-Hashimi, H. M. Extending the sensitivity of CEST NMR spectroscopy to micro-to-millisecond dynamics in nucleic acids using high-power radio-frequency fields. *Angewandte Chemie International Edition*. **59** (28), 11262-11266 (2020).
15. Hansen, D. F., Vallurupalli, P., Kay, L. E. Using relaxation dispersion NMR spectroscopy to determine structures of excited, invisible protein states. *Journal of Biomolecular NMR*. **41** (3), 113-120 (2008).
16. Lundström, P., Akke, M. Off-resonance rotating-frame amide proton spin relaxation experiments measuring microsecond chemical exchange in proteins. *Journal of Biomolecular NMR*. **32** (2), 163-173 (2005).
17. Lee, J., Dethoff, E. A., Al-Hashimi, H. M. Invisible RNA state dynamically couples distant motifs. *Proceedings of*

- the National Academy of Sciences of the United States of America*. **111** (26), 9485-9490 (2014).
18. Schnieders, R., Keyhani, S., Schwalbe, H., Fürtig, B. More than proton detection—new avenues for NMR spectroscopy of RNA. *Chemistry*. **26** (1), 102-113 (2020).
 19. Fürtig, B., Richter, C., Wöhnert, J., Schwalbe, H. NMR spectroscopy of RNA. *Chembiochem*. **4** (10), 936-962 (2003).
 20. Schlagnitweit, J., Steiner, E., Karlsson, H., Petzold, K. Efficient detection of structure and dynamics in unlabeled RNAs: The SELOPE approach. *Chemistry*. **24** (23), 6067-6070 (2018).
 21. Feyrer, H., Munteanu, R., Baronti, L., Petzold, K. One-pot production of RNA in high yield and purity through cleaving tandem transcripts. *Molecules*. **25** (5), 1142 (2020).
 22. Baronti, L., Karlsson, H., Marušič, M., Petzold, K. A guide to large-scale RNA sample preparation. *Analytical and Bioanalytical Chemistry*. **410** (14), 3239-3252 (2018).
 23. Brunelle, J. L., Green, R. In vitro transcription from plasmid or PCR-amplified DNA. *Methods in Enzymology*. **530**, 101-114 (2013).
 24. Borkotoky, S., Murali, A. The highly efficient T7 RNA polymerase: A wonder macromolecule in biological realm. *International Journal of Biological Macromolecules*. **118** (Pt A), 49-56 (2018).
 25. Arnaud-Barbe, N., Cheynet-Sauvion, V., Oriol, G., Mandrand, B., Mallet, F. Transcription of RNA templates by T7 RNA polymerase. *Nucleic Acids Research*. **26** (15), 3550-3554 (1998).
 26. Guillerez, J., Lopez, P. J., Proux, F., Launay, H., Dreyfus, M. A mutation in T7 RNA polymerase that facilitates promoter clearance. *Proceedings of the National Academy of Sciences of the United States of America*. **102** (17), 5958-5963 (2005).
 27. Kuzmine, I., Gottlieb, P. A., Martin, C. T. Binding of the priming nucleotide in the initiation of transcription by T7 RNA polymerase. *Journal of Biological Chemistry*. **278** (5), 2819-2823 (2003).
 28. Gholamalipour, Y., Karunanayake Mudiyansele, A., Martin, C. T. 3' end additions by T7 RNA polymerase are RNA self-templated, distributive and diverse in character - RNA-Seq analyses. *Nucleic Acids Research*. **46** (18), 9253-9263 (2018).
 29. Inoue, H., Hayase, Y., Iwai, S., Ohtsuka, E. Sequence-dependent hydrolysis of RNA using modified oligonucleotide splints and RNase H. *FEBS Letters*. **215** (2), 327-330 (1987).
 30. Wang, X., Li, C., Gao, X., Wang, J., Liang, X. Preparation of small RNAs using rolling circle transcription and site-specific RNA disconnection. *Molecular Therapy - Nucleic Acids*. **4**, e215 (2015).
 31. Karlsson, H., Baronti, L., Petzold, K. A robust and versatile method for production and purification of large-scale RNA samples for structural biology. *RNA*. **26** (8), 1023-1037 (2020).
 32. Hartmann, S. R., Hahn, E. L. Nuclear double resonance in the rotating frame. *Physical Review*. **128** (5), 2042-2053 (1962).
 33. Chiarparin, E., Pelupessy, I., Bodenhausen, G. Selective cross-polarization in solution state NMR. *Molecular Physics*. **95** (5), 759-767 (1998).
 34. Korzhnev, D. M., Orekhov, V. Y., Kay, L. E. Off-resonance R1ρ NMR studies of exchange dynamics in

- proteins with low spin-lock fields: an application to a Fyn SH3 domain. *Journal of the American Chemical Society*. **127** (2), 713-721 (2005).
35. Hansen, A. L., Nikolova, E. N., Casiano-Negroni, A., Al-Hashimi, H. M. Extending the range of microsecond-to-millisecond chemical exchange detected in labeled and unlabeled nucleic acids by selective carbon R1 ρ NMR spectroscopy. *Journal of the American Chemical Society*. **131** (11), 3818-3819 (2009).
 36. Duss, O., Maris, C., Schroetter, C. von, Allain, F. H.-T. A fast, efficient and sequence-independent method for flexible multiple segmental isotope labeling of RNA using ribozyme and RNase H cleavage. *Nucleic Acids Research*. **38** (20), e188-e188 (2010).
 37. Krähenbühl, B., Lukavsky, P., Wider, G. Strategy for automated NMR resonance assignment of RNA: application to 48-nucleotide K10. *Journal of Biomolecular NMR*. **59** (4), 231-240 (2014).
 38. LeBlanc, R. M., Longhini, A. P., Le Grice, S. F. J., Johnson, B. A., Dayie, T. K. Combining asymmetric ¹³C-labeling and isotopic filter/edit NOESY: a novel strategy for rapid and logical RNA resonance assignment. *Nucleic Acids Research*. **45** (16), e146 (2017).
 39. Parisien, M., Major, F. The MC-Fold and MC-Sym pipeline infers RNA structure from sequence data. *Nature*. **452** (7183), 51-55 (2008).
 40. Fürtig, B., Richter, C., Bermel, W., Schwalbe, H. New NMR experiments for RNA nucleobase resonance assignment and chemical shift analysis of an RNA UUCG tetraloop. *Journal of Biomolecular NMR*. **28** (1), 69-79 (2004).
 41. Keyhani, S., Goldau, T., Blümli, A., Heckel, A., Schwalbe, H. Chemo-enzymatic synthesis of position-specifically modified RNA for biophysical studies including light control and NMR spectroscopy. *Angewandte Chemie International Edition*. **57** (37), 12017-12021 (2018).
 42. Marchanka, A., Kreutz, C., Carlomagno, T. Isotope labeling for studying RNA by solid-state NMR spectroscopy. *Journal of Biomolecular NMR*. **71**, 151-164 (2018).
 43. Becette, O., Olenginski, L. T., Dayie, T. K. Solid-phase chemical synthesis of stable isotope-labeled RNA to aid structure and dynamics studies by NMR spectroscopy. *Molecules*. **24** (19), 3476 (2019).
 44. Zhang, X., Li, M., Liu, Y. Optimization and characterization of position-selective labelling of RNA (PLOR) for diverse RNA and DNA sequences. *RNA Biology*. **17** (7), 1009-1017 (2020).
 45. Roh, J. H. et al. Effects of preferential counterion interactions on the specificity of RNA folding. *The Journal of Physical Chemistry Letters*. **9** (19), 5726-5732 (2018).
 46. Juen, M. A. et al. Excited states of nucleic acids probed by proton relaxation dispersion NMR spectroscopy. *Angewandte Chemie German Edition*. **55** (39), 12008-12012 (2016).